This is a repository copy of *IoT focused VHF and UHF propagation study and comparisons*.

White Rose Research Online URL for this paper:
https://eprints.whiterose.ac.uk/174480/

Version: Published Version

White Rose
university consortium
Universities of Leeds, Sheffield & York

eprints@whiterose.ac.uk
https://eprints.whiterose.ac.uk/

ORIGINAL RESEARCH PAPER

IoT focused VHF and UHF propagation study and comparisons

D.P. Wright ⓘ | E.A Ball ⓘ

Department of Electronic and Electrical Engineering, Portobello Centre, University of Sheffield, Sheffield, UK

Correspondence

D.P. Wright, University of Sheffield, Department of Electronic and Electrical Engineering, Portobello Centre, Pitt Street, Sheffield, UK.
Email: dwright3@sheffield.ac.uk

Funding information

University of Sheffield, Grant/Award Number: phd funding; Engineering and Physical Sciences Research Council, Grant/Award Number: phd funding

Abstract

As the market for internet of things (IoT) is growing and due to Ofcom's decision to reassign parts of the very high frequency (VHF) spectrum in the UK for IoT use, a propagation study has been conducted using the newly released VHF spectrum and the currently commercially operated ultra-high frequency (UHF) spectrum, in order to compare and contrast the suitability of the VHF spectrum for IoT use. The authors conducted their study in a number of different environments (rural, suburban, urban and dense urban), with measurement equipment deployed in a manner suitable for a portable IoT use case. Results are presented in comparison to other propagation studies available in the literature and widely used propagation models such as the Hata model. Shadowing and noise are also measured and examined. It is found that current propagation models do not provide adequate predictions within the considered use case, but found it is possible to calculate log-distance based models that provide good predictions. Path-loss is found to be constantly lower at VHF than UHF, but radio frequency noise is consistently higher. The newly released spectrum is found to be suitable for IoT deployments in all the examined environments.

1 | INTRODUCTION

The internet of things (IoT) is a rapidly growing sector of communications technology, with 7 billion devices currently deployed and up to 22 billion devices expected to be deployed by 2025 [1]. With this large number of devices expected to be in use, it is easy to see how existing spectrum resources may become depleted. To alleviate this problem in the UK, the telecommunication's regulator Ofcom began consultations in September 2015, which led to the March 2016 approval for very high frequency (VHF) spectrum at 55–68 MHz, 70.5–71.5 MHz and 80–81.5 MHz to be re-purposed for use in IoT applications [2]. Ofcom is currently intending to use this re-purposed spectrum in rural settings, such as smart farming, but there is no reason this spectrum should not be considered for urban use.

In order to examine the use of this newly re-purposed spectrum, a propagation study will be conducted using a commercial off the shelf (COTS) software defined radio (SDR) based instrument previously developed and described by the authors of this paper in [3] and [4]. This instrument is specifically designed to operate within an IoT use case.

Current market leading IoT technologies such as LoRa and Sigfox use the short range devices (SRD) band at ∽869 MHz [5, 6]. To gauge the performance of the re-purposed band in relation to these current technologies, the propagation study will also cover SRD spectrum at ∽869 MHz. The work of authors will include comparisons between the measured and modelled propagation of the two bands, as well as the radio frequency (RF) noise measured and predicted.

Due to more favourable propagation characteristics, such as lower penetration loss and reduced scattering with longer wavelengths [7], lower VHF spectrum could be exploited for use in low power, high reliability communications systems [8].

The important contributions of the work of the authors to the literature are:

1. Provide an IoT focused propagation study at ∽70 MHz, which is a frequency not previously used for IoT
2. Provide comparisons between currently utilised IoT spectrum in the ∽869 MHz SRD band and the re-purposed ∽70 MHz band, and identifying comparative strengths and weaknesses.

3. Provide comparisons between International Telecommunication Union (ITU) predictions (for propagation, noise, shadowing and clutter) and an extensive set of real world measurements.
4. Provide new propagation models for the measured re-purposed ∽70 MHz band based on the log-distance path-loss model.

1.1 | Existing published propagation studies

The literature was reviewed for propagation studies involving VHF, ultra-high frequency (UHF) and IoT use cases. The relevant identified studies are described as follows.

Faruk et al. [9] describe a path-loss study focusing on the effects of terrain elevation and urban clutter. Multiple measurements are taken within urban and countryside environments at distances up to 33 km, using the VHF and UHF bands and compared to existing propagation models. TV transmitters were used as the transmit signal (TX) for the study, so antenna heights of 100 to 340 m and TX power of 1–7 kW are considered. The most accurate model was found to be the ILORIN model, which is a modification of the Hata-Davidson model based on empirical measurements previously taken in and around Ilorin, Nigeria. As the study was conducted in this area, it is no surprise that this specially tailored model worked best. It was also discovered that changes in terrain elevation introduce significant errors between the path-loss predictions of all the examined models and the actual measurements.

Andrusenko et al. [10] studied urban short range (less than 1 km) VHF (30–88 MHz) propagation, mainly focusing on indoor and indoor to outdoor propagation. Further, a propagation model called general urban path-loss (GUPL) is developed based on the log-distance model, floor attenuation model and experimentally collected data, some improved ideas proposed previously by Devasirvatham et al. [11]. This model is shown in (1), and the parameters calculated for outdoor urban canyon propagation are: power exponent = 2.2, path-loss exponent = 1.8, attenuation constant = 0.06 dB/m and floor attenuation factor = 0. The number of measurements for some considered scenarios is as low as 3 measurements over a 90 m TX (transmitter) to RX (receiver) separation, which is a very low number to use for estimating model parameters in these scenarios. This model will be compared to measurements taken in our experiments.

$$\text{GUPL(dB)} = -10\log_{10}\left(\left[\frac{\lambda}{4\pi d_0}\right]^{\beta}\right) + 10n\log_{10}\left(\frac{d}{d_0}\right)$$
$$+ \alpha d + \text{FAF}$$

$$(1)$$

where:

GUPL(dB) = Path-loss (dB)
λ = Wavelength (m)
d_0 = Reference distance in the far field region (m)
β = Power component
n = Path-loss exponent
d = Distance between TX and RX (m)
α = Attenuation constant (dB/m)
FAF = Floor attenuation factor, based on the number of building floors a signal passes through (dB)

A smart meter focused outdoor to indoor propagation study was conducted by Fuschini et al. [12] at a frequency of 169 MHz, in order to match the European standard defined SRD band frequency range for smart meters of 169.4 to 169.475 MHz [13]. A continuous wave (CW) signal with an effective isotropic radiated power (EIRP) of 27 dBm was used in the study, this is the maximum power level allowed by the standard [13]. The TX was provided by a signal generator with external amplifier and then fed to a yagi antenna. A directional antenna such as this does not fit the smart meter use case and would have caused fewer reflections than a less directional antenna such as a dipole, which could affect the measured propagation. The authors also investigate losses associated with propagation through the fabric of a building (building penetration loss) and losses associated with the positioning of the meter within the building, such as within a metal enclosure (installation loss). It was found that building penetration loss could be represented by a log-normal distributed variable, with an average of 7.5 dB and a standard deviation of 4.5 dB. Installation loss was found to be 7 dB when installed within a metal grid and 13 dB when installed in a basement.

Ayadi et al. [14] describe a UHF propagation study that collects path-loss data in order to train a neural network to produce a path-loss model, which can then be compared to other established models. This method was found to be able to produce a model which was compared favourably with the established models, but it had higher processing time and memory requirements when used.

Sarkar et al. [15] analyse short range global system for mobiles (GSM) signal propagation between 900 and 1800 MHz. Environments considered were urban, suburban, industrial and over water. A measurement campaign was conducted using GSM base stations for TX and GSM mobile phone handsets for RX, with measurement locations recorded by GPS. It is concluded that at the measured frequencies the propagation over ground is the dominant influence over path-loss, with environmental concerns such as trees and buildings producing a secondary effect.

Dagefu et al. [8] analyse short range, low VHF (∽40 MHz), near ground indoor and indoor-outdoor propagation at distances of up to 200 m. Also, it focuses on measurements of phase and channel transfer function. It is determined that the low VHF band is a good choice for low power, low data-rate and short range communications with simple channel models being able to reasonably predict real world performance.

El Chall et al. [16] investigated RF propagation for outdoor (urban and rural) and indoor LoRaWAN deployments in the 868 MHz band. A commercial Pycom LoRa equipped transmitter was used as a portable TX source, and a commercial Kerlink LoRa gateway was used for RX. The RX gateway provides received signal strength and signal-to-noise ratio as the location of the TX is moved within each of the different

environments. Parameters for the LoRa transmission were set to provide the best sensitivity and therefore lowest data rate, making the measurements only applicable to best case scenario propagation LoRa deployments. Measurements confirmed that the shadowing observed fits a Gaussian zero mean distribution, as is widely used for modelling. New models were developed, including corrections for antenna height. A model for outdoor propagation was developed and is given in (2).

$$PL = 10n\log_{10}(d) + PL_0 + L_b\log_{10}(b_{ED}) + X_\sigma \quad (2)$$

where:

PL = Path-loss (dB)
n = Path-loss exponent
PL_0 = Path-loss at reference distance
d = Distance between TX and RX (km)
L_b = Additional loss due to RX antenna height (dB)
b_{ED} = RX antenna height (m)
X_σ = Log-normal shadowing (dB)

Calculated parameters for outdoor campus environments are given in [16] as $n = 3.12$, $PL_0 = 140.7$, $L_b = -4.7$ and $\sigma = 9.7$. For Outdoor urban they are $n = 4.179$, $PL_0 = 102.86$, $L_b = -6.3$ and $\sigma = 7.2$. For outdoor rural they are $n = 3.033$, $PL_0 = 111.75$, $L_b = -6.65$ and $\sigma = 6.4$. This model will be compared to measurements taken in our work.

Sandoval et al. [17] examined path-loss based on the received signal strength indicator (RSSI) of deployed IoT nodes of IEEE 802.15.4 standard at 2.4 GHz. The study compares RSSI readings with readings from a vector network analyser (VNA) and quantifies and accounts for errors made by the nodes in RSSI readings. Once the errors were accounted for, readings from the RSSI were found to be in close agreement with VNA derived readings, showing that this method can provide a low-cost method of conducting propagation studies.

Hejselbæk et al. [18] study the propagation for IoT devices deployed near to ground in a forest environment at a frequency of 917.5 MHz. Measurements were found to be in close agreement to predictions made by the two ray model when corrected for clutter loss. Measurements also showed agreement with the model previously proposed by Tewari et al. [19]

Wang et al. [20] use an on body to on body device propagation study to investigate and improve the security of IoT devices, showing results which can be a motivating factor for IoT propagation studies.

1.2 | Established propagation models

The propagation measurements taken by the authors will be compared with predictions taken from currently available propagation models. This will enable these models to be validated for the frequencies and environments studied here, or to establish the requirement for a new model to be developed. The models used are listed as follows:

- **Free Space Path-loss** [21]. Included to provide a baseline comparison using the simplest way to predict propagation.
- **Two Ray Model** [22]. Included to provide a slightly more complicated comparison and investigate the accuracy of modelling propagation in an urban or suburban environment with only two propagated rays (one line of sight, one reflected). Can an urban canyon be accurately modelled using only two dominant rays?
- **Hata Urban** [22]. A widely used empirical model for urban mobile communications, valid for frequencies from 150 to 1500 MHz, distances over 1 km and TX antenna heights over 30 m. This model is not valid for the use case here (distances and antenna heights are much shorter), but it is included to assess the use case against established, currently utilised models for urban deployments.
- **Hata Suburban** [22]. Is an extension of the Hata model for suburban deployments.
- **Models identified in the literature review** developed by Andrusenko et al. [10] (GUPL) and El Chall et al. [16] identified in Section 1.1.

1.3 | Calculating a log-distance propagation model

The log-distance propagation model given in (3) [22] is an established way to produce environment specific models in which the path-loss increases with the log of the distance between the TX and the RX according to specifically tailored variables. This technique will be used with the measurements taken in this study to provide a new model for comparison to the existing models.

$$P_L(dB) = K + 10\gamma\log_{10}(d) + X_{\sigma dB} \quad (3)$$

where

$P_L(dB)$ = Path-loss (dB)
K = A constant, depending on antenna characteristics and average channel attenuation [22]
γ = Path-loss exponent
d = Distance between TX and RX (m)
$X_{\sigma dB}$ = Log-normal random variable with standard deviation of σ (dB)

Linear regression to the measurements taken is used to provide figures for K and γ in (3), further details can be found in the author's previous paper [4]. The log-normal random variable relates to shadowing and will be dealt with in Section 1.4.

1.4 | Shadowing

A common way to represent shadowing within propagation measurements is using a random variable with a log normal distribution of a specific standard deviation, this is represented in (3) by the variable $X_{\sigma dB}$.

The International Telecommunications Union-Radiocommunications Sector (ITU-R) provide a method for prediction of shadowing in large flat urban areas in their recommendation ITU-R P.1406-2 [23] which is stated to be valid from 100 MHz to 3 GHz, and this method is given in (4).

$$\sigma_L = 5.25 + 0.42 \log_{10}\left(\frac{f}{100}\right) + 1.01 \log_{10}^2\left(\frac{f}{100}\right) \quad (4)$$

where

σ_L = Standard deviation for a given length (dB)
f = Frequency (MHz)

This method is used to provide predictions which can be compared to the measurements taken in order to verify the validity of the method's possible use for the re-purposed VHF bands examined here. Using the model, the following shadowing standard deviation predictions were made: σ_L = 5.2 dB at 71 MHz and σ_L = 6.5 dB at 869.525 MHz.

In order to obtain the measured shadowing from the propagation measurements taken, each measurement is compared with the linear regression model (excluding the shadowing variable) shown in (3) at the same distance from the TX as the measurement was taken. This can be seen in (5) [22]

$$\sigma_{\mathrm{dB}} = \sqrt{\frac{1}{n}\sum_{i=1}^{n}\left[M_{\mathrm{measured}}(d_i) - M_{\mathrm{model}}(d_i)\right]^2} \quad (5)$$

where

σ_{dB} = Standard deviation of the shadowing (dB)
n = Number of measurements taken
$M_{\mathrm{measured}}(d_i)$ = Propagation measurement at a given distance
$M_{\mathrm{model}}(d_i)$ = Propagation prediction using linear regression at a given distance

This gives the shadowing standard deviation, allowing the model described in (3) to be completed. Further details can be found in the author's previous paper [4].

2 | FIELD MEASUREMENTS

The instrument previously developed and discussed by the authors in [3] and [4] is used to take path-loss measurements. This instrument consists of a SDR receiver, attached to a Raspberry Pi and a GPS receiver. A sleeved dipole (2.15 dBi gain) is used for UHF reception and a Helical antenna (−14 dBi gain) is used for VHF reception, in order to represent the small, low efficiency antennas common in IoT applications. TX is provided by a custom designed VHF transmitter and a Silicon Labs Si106x wireless microcontroller unit development kit [24] for UHF, both transmitters are connected to dipole antennas (2.15 dBi gain) and transmit a CW signal with a conducted power to the antennas of +9.5 dBm, giving an EIRP of +11.65 dBm. Further details of the construction and calibration of the SDR-based instrument can be found in Wright and

Ball [4]. The instrument is carried in a car around a predetermined area of interest; measurements of RX power and GPS location are recorded in order to be processed in to pathloss information. It is likely that the measurements will be a rich mixture of Line-of-sight (LOS) and Non-Line-of-sight (NLOS), due to the nature of the trials. It is not practical to try and split the measured data on a point-by-point basis to ascribe it to LOS or NLOS. Due to licences obtained from Ofcom, the instrument operates at 71 MHz and 869.525 MHz, respectively.

The instrument measures RF noise by examining the Fast Fourier transform (FFT) it has produced of the measured spectrum. A peak detection algorithm is performed on the FFT and all FFT bins where a peak has been detected are assumed to contain a signal and are discarded, the remaining bins are assumed to contain no signal and only noise. These bins are then averaged across the FFT to give a value in dBm for the average noise in the measured bandwidth. The instrument records 5000 samples taken at a sampling frequency of 2.048 MHz, which gives a resolution bandwidth of 409.6 Hz for the FFT.

The following subsections provide details of the areas where measurements are taken, including location coordinates for the transmitters, antenna heights and a map of the areas with individual measurement locations indicated. Multiple diverse locations were chosen for measurements in order to provide information across dense urban, urban, suburban and rural environments. As it was not possible to have the TX antennas deployed at the same height in all environments, and moreover a street level deployment was not practical in a city centre and no tall buildings were available in the rural environment, the study was restricted to accessible and secure locations only.

2.1 | Rural (Burniston)

Measurements were taken in and around the rural village of Burniston, near Scarborough, UK. The area consists of farm land, woods and small residential settlements. A map of the area with measurement and TX locations can be seen in Figure 1. The TX is located at the approximate coordinates −0.449, 54.323 with an antenna height of 2 m. The instrument conducted 725 measurements from which 89 detections of the 71 MHz signal and 134 detections of the 869.525 MHz signal were registered.

Calculated path-loss measurements for VHF and UHF are shown in Figure 2 along with the calculated log-distance model and shadowing standard deviation given in (6) and (7).

The RF noise measured in the area during the test is shown in Figure 3

$$P_{\mathrm{L71}}(\mathrm{dB}) = 64.2 + 13.8 \log_{10}(d) + X_{6.1\ \mathrm{dB}} \quad (6)$$

$$P_{\mathrm{L869}}(\mathrm{dB}) = 92.8 + 13.4 \log_{10}(d) + X_{6.5\ \mathrm{dB}} \quad (7)$$

The calculated path-loss exponent for the fitted rural models in (6) and (7) show a result lower than 2. This is very unusual, but can occur with constructive ray interference and has been seen elsewhere within buildings [7] and in vehicle to

FIGURE 1 Locations of TX and Measurements in the Buriston area. Underlying map ©OpenStreetMap contributors www.openstreetmap.org/copyright
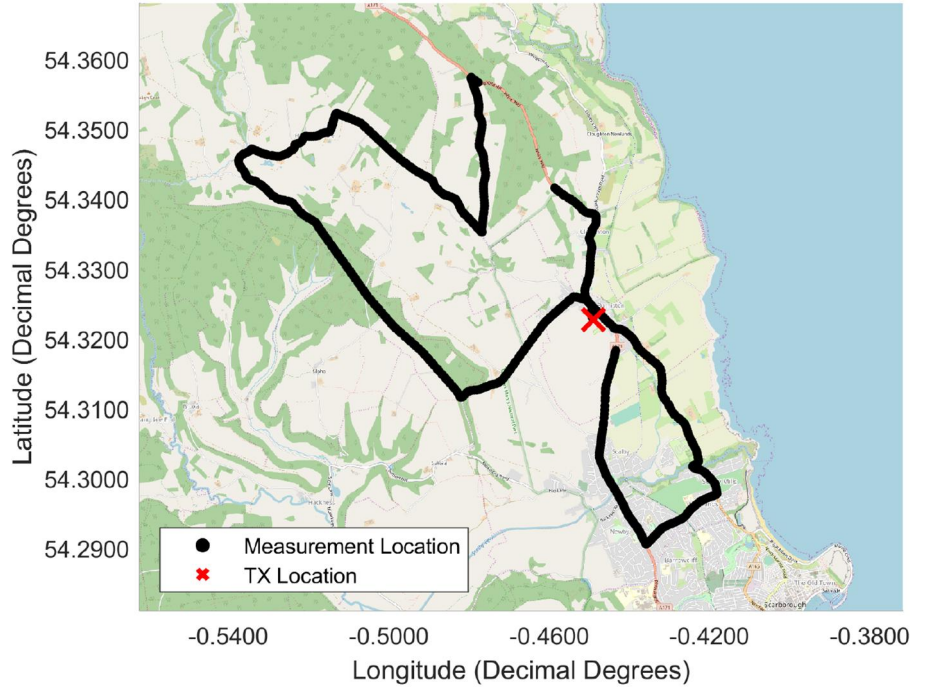
vehicle propagation studies [25]. We also note that the fixed loss parameter K for the rural models is very high, suggesting the propagation was subject to very significant fixed loss, possibly skewing the model and resulting in the lower slope parameter. However, the model does have a good overall fit to the measured data, as seen by the R^2 values in Tables 1 and 2. Care should be taken in field tests to try and minimise any initial deployment fixed losses, to reduce this skewing of the fitted models. The high fixed loss also led to less signal detection's being registered for both frequencies in this environment, when compared to the other environments in this section.

2.2 | Suburban (Wakefield)

Measurements were taken around a suburban area of Wakefield, UK. The area consists of residential, parkland and low rise warehouses. A map of the area with measurement and TX locations can be seen in Figure 4. TX is located at the approximate coordinates −1.505, 53.715 with an antenna height of 4 m. The instrument conducted 2101 measurements from which 826 detections of the 71 MHz signal and 901 detections of the 869.525 MHz signal were registered.

Calculated path-loss measurements for VHF and UHF are shown in Figure 5 along with the calculated log-distance model and shadowing standard deviation given in (8) and (9).

The RF noise measured in the area during the test is shown in Figure 6

$$P_{L71}(dB) = 8.5 + 34.0 \log_{10}(d) + X_{5.5 \text{ dB}} \quad (8)$$

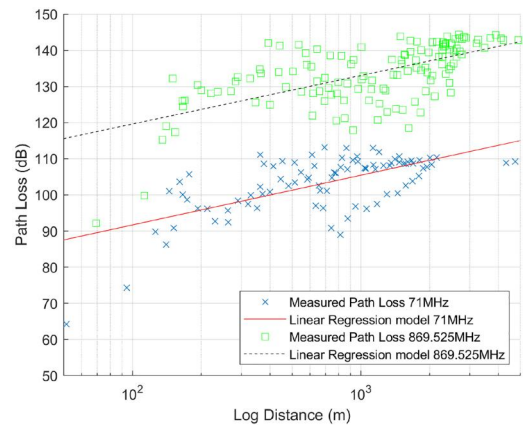**FIGURE 2** Burniston propagation results for VHF and UHF

$$P_{L869}(dB) = 36.5 + 33.2 \log_{10}(d) + X_{8.0 \text{ dB}} \quad (9)$$

2.3 | Urban (Sheffield)

Measurements were taken in and around the city centre of Sheffield, UK. The area consists of retail, high rise residential and low rise industrial. A map of the area with measurement and TX locations can be seen in Figure 7. The TX is located at the approximate coordinates −1.477, 53.382 with an antenna height of 10 m. The instrument conducted 999 measurements from which 280 detections of the 71 MHz signal and 418 detections of the 869.525 MHz signal were registered.

Calculated path-loss measurements for VHF and UHF are shown in Figure 8 along with the calculated log-distance model and shadowing standard deviation given in (10) and (11).
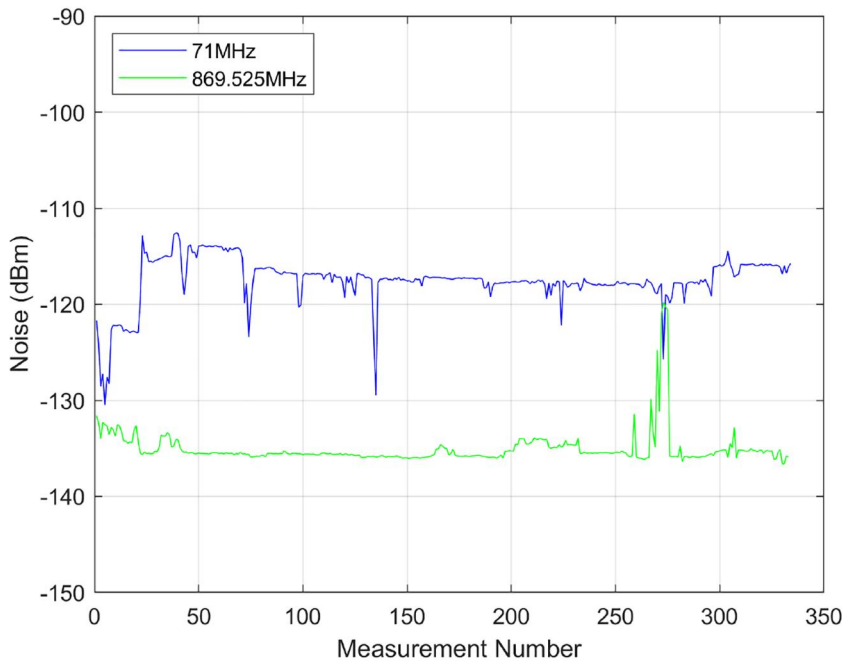
FIGURE 3 Burniston noise measurements for VHF and UHF

TABLE 1 Summary of The calculated log-distance parameters at VHF

Environment	γ	K	(dB)	R^2
Rural	1.38	64.2	6.1	0.43
Sub-urban	3.40	8.5	5.5	0.80
Urban	3.42	16.8	8.1	0.66
Dense urban	2.11	43.7	8.9	0.38

TABLE 2 Summary of the calculated log-distance parameters at UHF

Environment	γ	K	(dB)	R^2
Rural	1.34	92.8	6.5	0.41
Sub-urban	3.32	36.5	8.0	0.66
Urban	3.89	19.1	7.9	0.64
Dense urban	2.74	48.9	7.9	0.53

The RF noise measured in the area during the test is shown in Figure 9

$$P_{L71}(dB) = 16.8 + 34.2 \log_{10}(d) + X_{8.1\ dB} \qquad (10)$$

$$P_{L869}(dB) = 19.1 + 38.9 \log_{10}(d) + X_{7.9\ dB} \qquad (11)$$

2.4 | Dense urban (Leeds)

Measurements were taken in and around the city centre of Leeds, UK. The area consists of retail, commercial and high rise residential. The area was chosen as dense urban over the Sheffield area due to the presence of many more tall buildings and the city's higher population. A map of the area with measurement and TX locations can be seen in Figure 10. The TX is located at the approximate coordinates −1.536, 53.794 with an antenna height of 20 m. The instrument conducted 1248 measurements from which 503 detections of the 71 MHz signal and 517 detections of the 869.525 MHz signal were registered.

Calculated path-loss measurements for VHF and UHF are shown in Figure 11 along with the calculated log-distance

model and shadowing standard deviation given in (12) and (13).

The RF noise measured in the area during the test is shown in Figure 12

$$P_{L71}(dB) = 43.7 + 21.1 \log_{10}(d) + X_{8.9\ dB} \qquad (12)$$

$$P_{L869}(dB) = 48.9 + 27.4 \log_{10}(d) + X_{7.9\ dB} \qquad (13)$$

Tables 1 and 2 show a summary of the path-loss exponent (γ), channel constant (K), shadowing (σ) and the R^2 fit for the straight line component of each model in the different environments.

3 | RESULTS

The measurements taken, which are described in Section 2 are now analysed here. Attention will be directed to path-loss measurements and their comparisons with model predictions in Section 3.1, the measured shadowing and predictions in Section 3.2, the measured noise in Section 3.3 and the effects of correcting free space and two ray models for extra clutter loss (including knife-edge diffraction) on the prediction accuracy of these models in Section 3.4.

FIGURE 4 Locations of TX and Measurements in Wakefield. Underlying map ©OpenStreetMap contributors www.openstreetmap.org/copyright
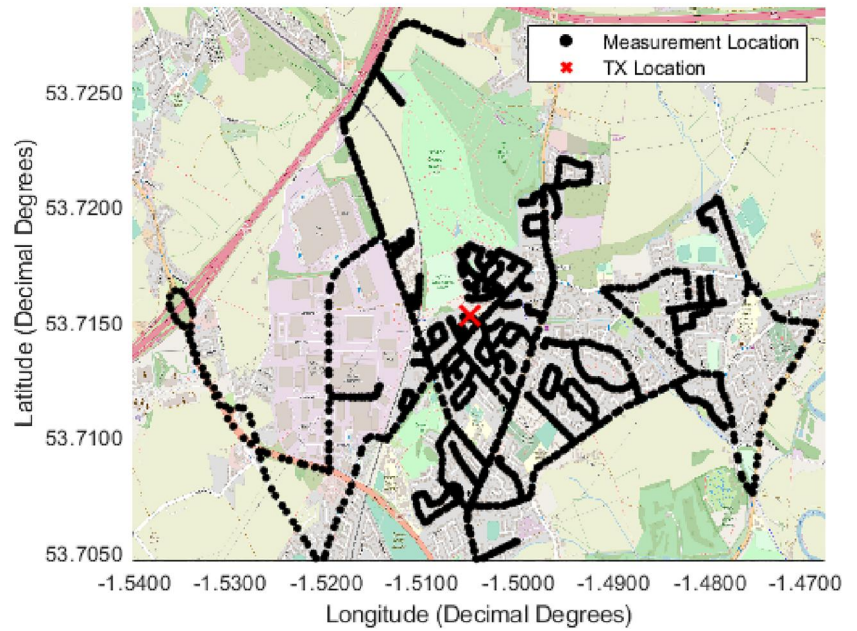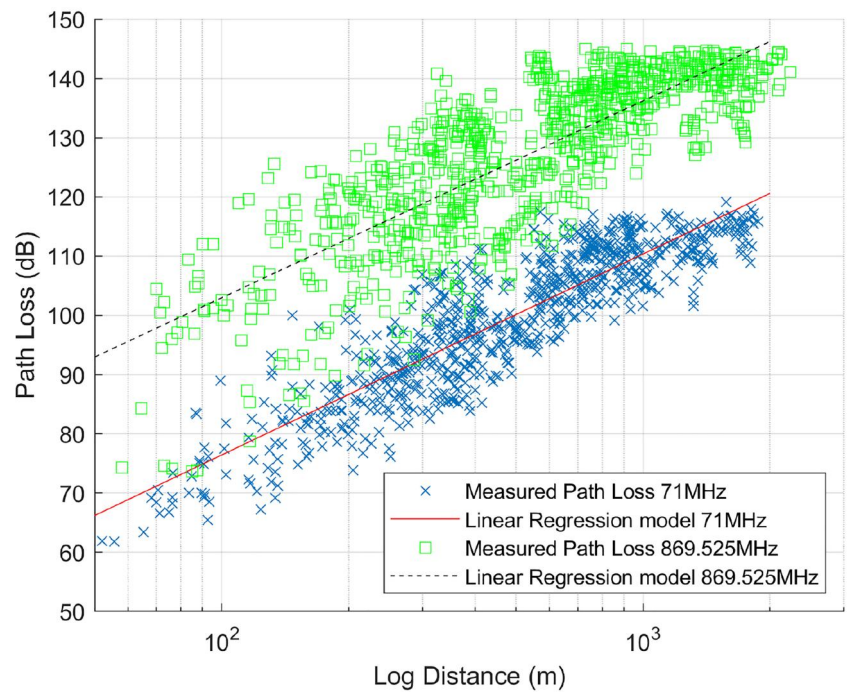

FIGURE 5 Wakefield propagation results for VHF and UHF

3.1 | Path-loss

The measurements and calculated models from Section 2 are compared with the established propagation models discussed in Section 1.2. The root mean squared error (RMSE) between the predictions and the measurements (E_{RMS}) are given in Table 3 for Rural Burniston, Table 4 for suburban Wakefield, Table 5 for urban Sheffield and Table 6 for dense urban Leeds.

Table 3 shows the calculated model produced by the authors' work best matches the rural measurements. No standard

models produce good predictions at VHF or UHF, though the predictions are significantly better at VHF.

Table 4 again shows that our calculated model best fits the suburban measured data at VHF and UHF. Two-Ray, Hata Urban and Hata Suburban produce comparable results to our model at VHF. This is surprising because the Hata models are not recommended for use in the VHF frequency examined here. Hata models are recommended for use in the UHF frequency, so a better performance would be expected from the models at UHF than VHF. No other standard model
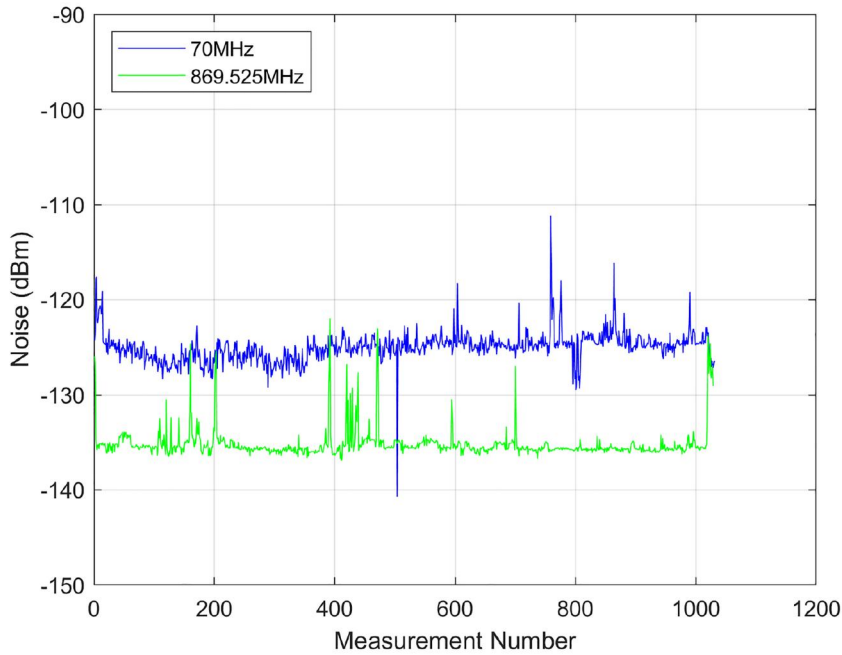
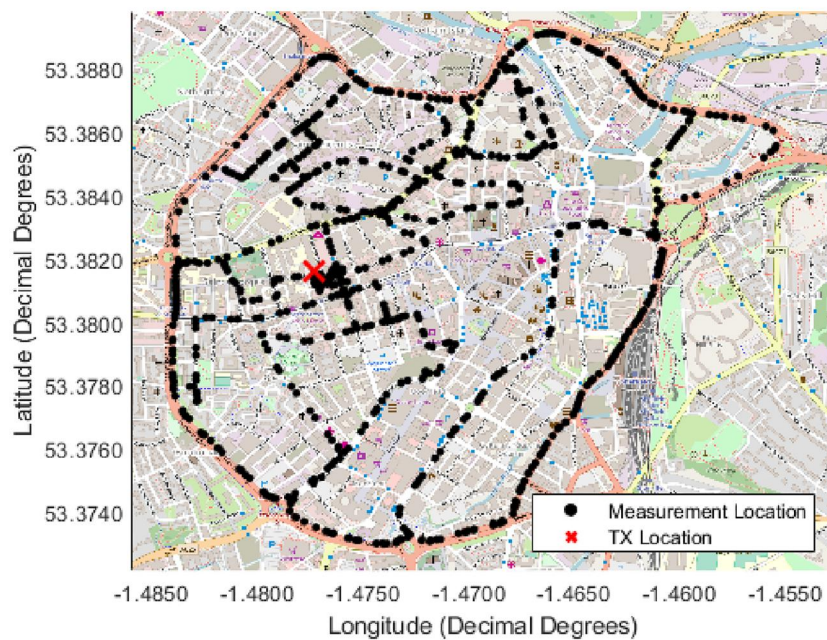**FIGURE 6** Wakefield noise measurements for VHF and UHF

FIGURE 7 Locations of TX and Measurements in Sheffield. Underlying map ©OpenStreetMap contributors www.openstreetmap. org/copyright

produces good results at either frequency, though again the predictions are better at VHF.

Table 5 shows that our calculated model gives the best fit to the urban measurement data at VHF and UHF. No standard model produces good results at either frequency, though again the predictions are better at VHF.

Table 6 once again shows that our calculated model produces predictions that best fit the dense urban measured data. No standard model produces good results at either frequency, though again the predictions are better at VHF.

It is perhaps not surprising that our calculated log-distance model performed best in all environments at both VHF and UHF, and this model was directly based on the measured results for each environment. It is, however, surprising that the Hata Urban and Suburban models consistently performed better outside their stated frequency range (VHF) than within (UHF). The GUPL and El Chall models both failed to produce accurate results even though they are based on measurements from similar environments, which suggests that a model that is very tailored to a particular place may not transfer very well to other places, even when the environment is similar.

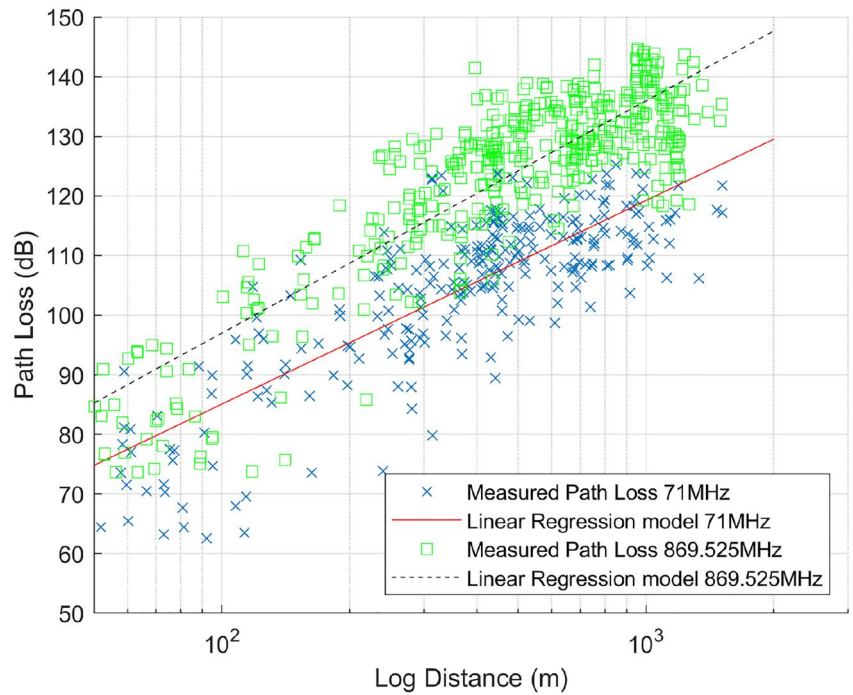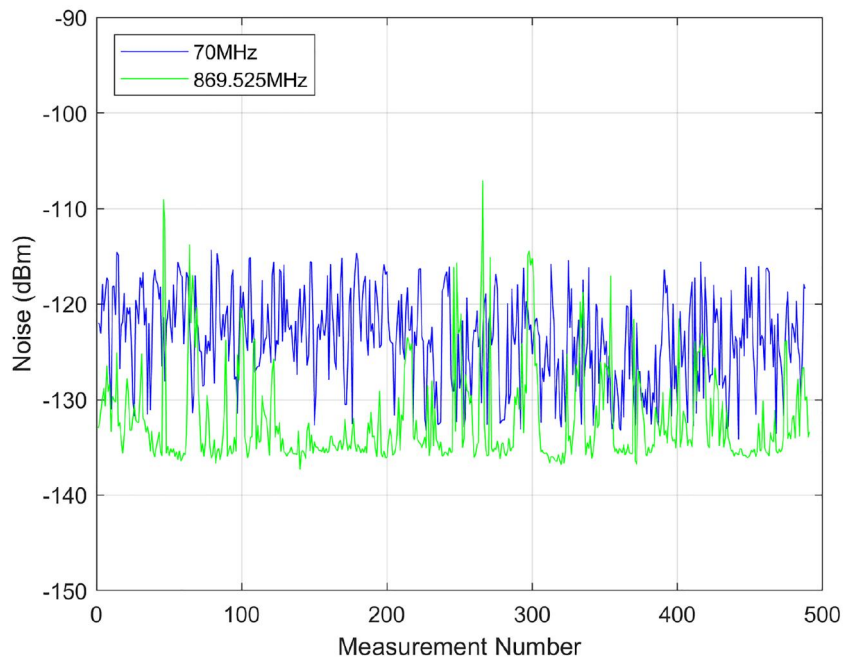**FIGURE 8** Sheffield propagation results for VHF and UHF

FIGURE 9 Sheffield noise measurements for VHF and UHF

The calculated log-distance path-loss models for both frequencies in all locations are compared in Figure 13. This shows that path-loss is consistently lower at VHF than at UHF. This is a expected behaviour and shows that VHF retains an advantage for long distance communications even in urban areas when using the use case set out in this study. At both VHF and UHF the loss for the urban environment is very high, which is due to a very high fixed loss (K) present in the data, with then only a slight fitting slope

needed. This can possibly be attributed to the deployment of the TX very close to a building in an area surrounded by trees.

Table 7 shows the measured path-loss exponents of the calculated log-distance models that were produced for both frequencies in all environments. Expected behaviour would be to see higher path-loss exponents for UHF over VHF within each environment and also for path-loss exponents to increase when moving to a more cluttered environment.
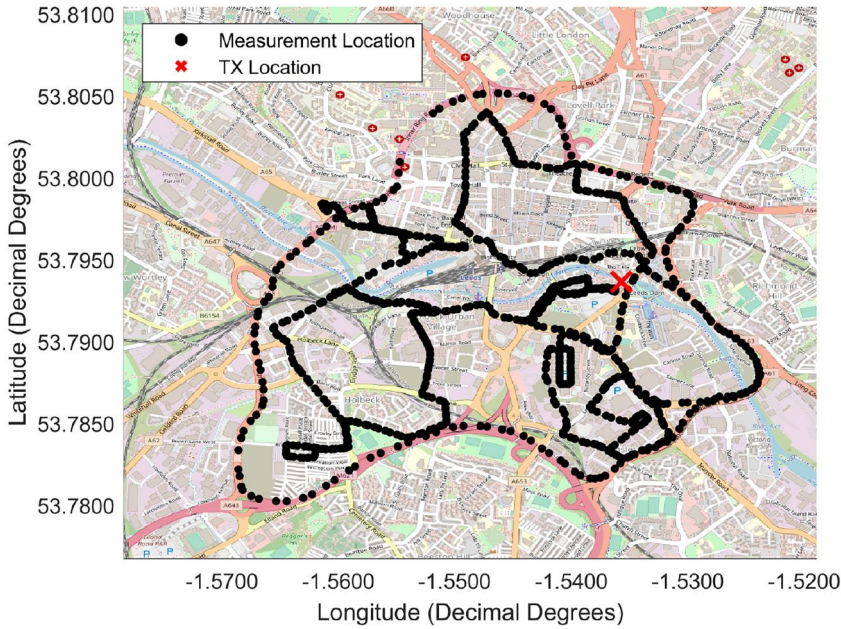
FIGURE 10 Locations of TX and measurements in Leeds. Underlying map ©OpenStreetMap contributors www.openstreetmap.org/copyright
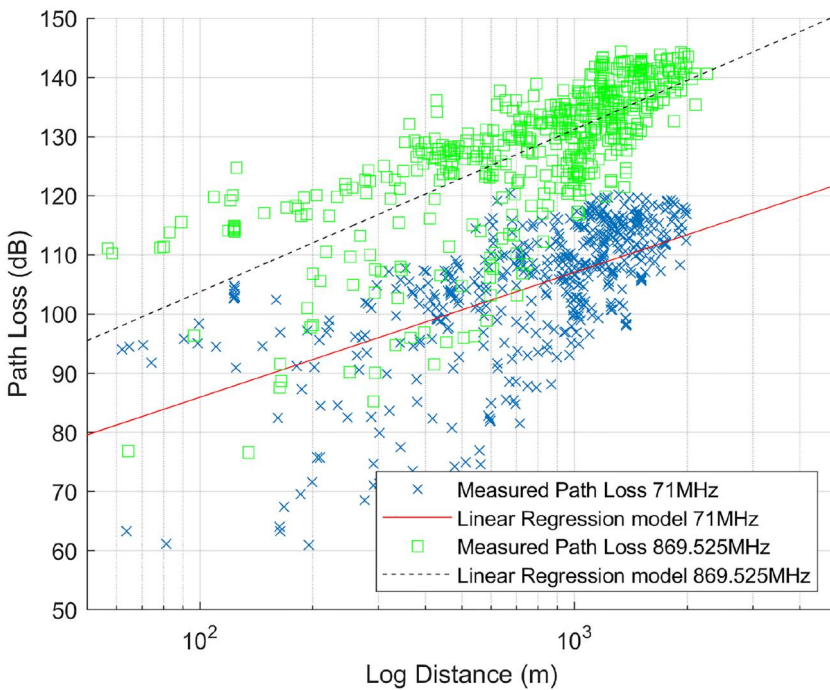

FIGURE 11 Leeds propagation results for VHF and UHF

However, the actual behaviour seen with the measurements show that in both rural and suburban environments the path-loss exponents are roughly similar at VHF and UHF. For environments with more clutter the path-loss exponent does tend to increase as predicted, except for dense urban. This can be attributed to the high antenna height use in the Leeds test, which is twice as high as the urban test antenna, placing it above much of the surrounding clutter and producing a scenario with much better propagation characteristics than the tests with antennas much closer to ground or located amongst a much taller clutter.

3.2 | Shadowing

The measured shadowing is compared to the prediction given by the ITU recommendation ITU-R P.1406-2 [23] discussed in Section 1.4. The log-normal shadowing standard deviation values for 71 and 869.525 MHz within each test area are given in Table 8. El Chall et al. [16] also provide predictions for shadowing in LoRa deployments as part of their model, campus = 9.7 dB, urban = 7.2 dB and rural = 6.4 dB.

The predictions given by the ITU are a little lower than the measurements, and at VHF, the measurements differ by the
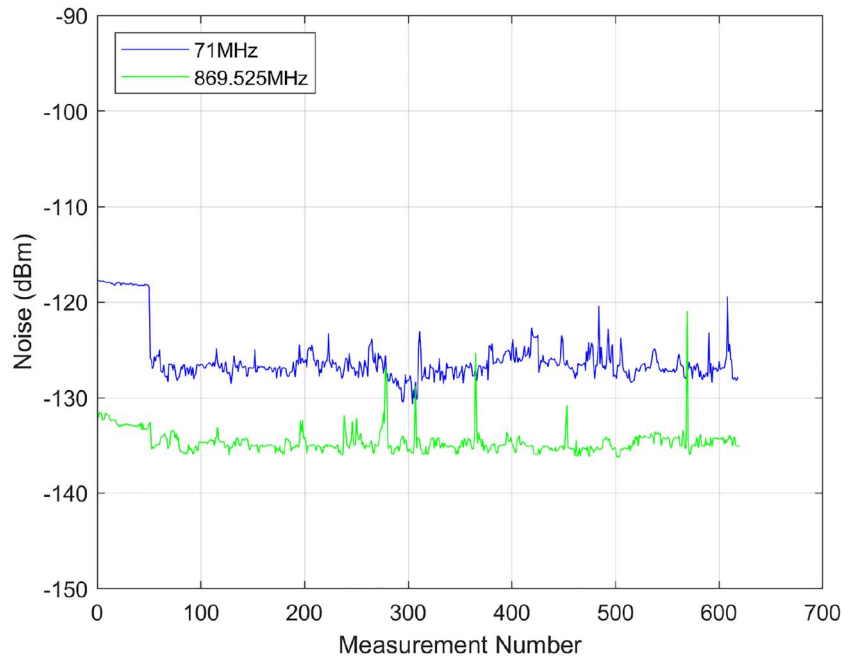
FIGURE 12 Leeds noise measurements for VHF and UHF

TABLE 3 RMSE Between Measurements and Established Models Predictions in the Rural Environment

	E_{RMS} (dB)	
Model	VHF	UHF
Free space	37.6	63.7
Two-ray	11.9	24.9
Hata urban	13.4	22.5
Hata suburban	13.0	27.3
GUPL	59.8	72.4
El Chall	-	24.5
Calculated model	6.1	6.5

TABLE 4 RMSE between measurements and established models predictions in the suburban environment

	E_{RMS} (dB)	
Model	VHF	UHF
Free Space	37.2	63.8
Two-Ray	9.8	34.6
Hata Urban	6.6	29.8
Hata Suburban	10.4	35.3
GUPL	21.8	37.0
El Chall	-	40.4
Calculated model	5.5	8.0

TABLE 5 RMSE between measurements and established models predictions in the urban environment

	E_{RMS} (dB)	
Model	VHF	UHF
Free Space	44.6	60.8
Two-Ray	26.6	39.9
Hata Urban	18.7	31.9
Hata Suburban	24.0	37.4
GUPL	25.9	33.0
El Chall	-	40.4
Calculated model	8.1	9.0

TABLE 6 RMSE between measurements and established models predictions in the dense urban environment

	E_{RMS} (dB)	
Model	VHF	UHF
Free Space	38.6	61.5
Two-Ray	21.4	43.0
Hata Urban	13.3	33.2
Hata Suburban	17.5	38.7
GUPL	67.2	28.3
El Chall	-	39.1
Calculated Model	8.9	7.9

following; rural = 0.9 dB, suburban = 0.3 dB, urban = 2.9 dB and dense urban = 3.7 dB; at UHF, the measurements differ by the following; rural = 0.0 dB, suburban = 1.5 dB, urban = 1.4 dB and dense urban = 1.4 dB. Considering that the ITU prediction is for flat urban areas and not all areas measured were flat or urban,

some deviations from the predictions were expected. Table 9 shows the variation of the height above sea-level for the measurements locations.
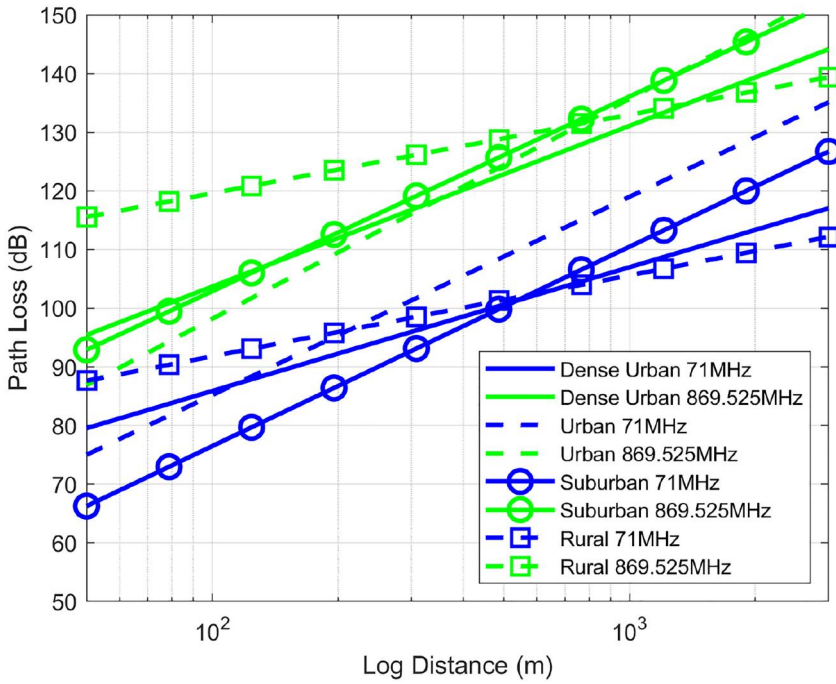
TABLE 7 Comparison of path-loss exponents from the calculated model for VHF and UHF in all environments

Environment	VHF (γ)	UHF (γ)
Rural	1.38	1.34
Suburban	3.40	3.32
Urban	3.42	3.89
Dense urban	2.11	2.74

For VHF, measurements show greater shadowing in rural areas than suburban, but shadowing is shown to increase as the urban environment increases in density, as expected. UHF measurements show lower shadowing for rural areas, but there is consistent shadowing as the urban density increases, meaning the increase in density has no further effect on shadowing. UHF measurements match well with the measurements made by El Chall et al. for LoRa deployments. Shadowing values are very similar at both VHF and UHF, except for the suburban environment, no frequency shows a clear advantage over the other.

3.3 | Noise

The average noise level and the standard deviation of this average for each environment and frequency are compared here, which is shown in Table 10. All noise measurements are made within a 409.6-Hz bandwidth.

At VHF, the average noise level roughly increases as the density of human activity increases from rural to dense urban, which suggests that the presence of more electronic devices and human activity increases the noise in the environment. At UHF, the average noise level does not increase in the same way and is constant across the environments, suggesting that the noise may not be as dependent on human activity. By inspecting the standard deviation results in Table 10 and Figures 3, 6, 9 and 12 it is possible to see that there is a greater variation in the noise measurements at both frequencies within the urban environment than within any other in environment. The measurements for the urban environment were performed during the normal working day, whereas the other environments were measured outside these times at weekends and evenings. This suggests that the higher human activity during the work day may create a more diverse RF environment and add a time-dependant factor to the levels of noise present in these environments.

3.4 | Extra clutter Loss

The ITU provides a model for the prediction of extra loss due to clutter, including knife-edge diffraction, in ITU-R P.2108-0 [26] which is shown in (14) and (15). The model is valid for terminals deployed below the level of the representative clutter height at frequencies between 30 MHz and 3 GHz.

By changing the value for representative clutter height between the values recommended by the ITU, 10 m for rural and suburban, 15 m for urban and 20 m for dense urban [26], it is possible to calculate the extra loss predicted in each environment. This extra loss can be added to the free space path-loss and two ray model to act as a form of correction factor to make these models more accurate to the measured data. Table 11 shows the extra clutter loss results predicted by the ITU model.

TABLE 8 Observed and Predicted Shadowing Standard Deviation

Frequency	ITU Prediction (dB)	Rural (dB)	Suburban (dB)	Urban (dB)	Dense urban (dB)
VHF	5.2	6.1	5.5	8.1	8.9
UHF	6.5	6.5	8.0	7.9	7.9

Abbreviation: ITU, International Telecommunication Union.

TABLE 9 Height of the recorded measurements above sea-level in each environment

	Mean (m)		Standard deviation (m)		Maximum (m)		Minimum (m)	
Environment	VHF	UHF	VHF	UHF	VHF	UHF	VHF	UHF
Rural	66.0	79.0	27.2	36.9	197.3	186.4	42.4	36.9
Suburban	76.4	73.7	10.2	14.6	99.7	106.4	26.5	23.1
Urban	84.5	77.1	21.1	20.4	154.7	158.3	47.9	47.2
Dense urban	37.9	37.4	10.8	9.7	82.7	71.5	11.3	4.9

TABLE 10 Analysis of the Noise Measured in Each Environment

	Mean (dBm)		Standard deviation (dBm)	
Environment	VHF	UHF	VHF	UHF
Rural	−119	−135	3.2	1.0
Suburban	−125	−135	1.4	1.3
Urban	−123	−133	4.6	3.3
Dense urban	−127	−135	1.6	1.1

$$A_h = \begin{cases} J(\nu) - 6.03 & \text{for all Urban} \\ -K_{h2} \log_{10}(h/R) & \text{for Rural} \end{cases} \quad (14)$$

where:

A_h = Additional loss due to clutter (dB)

$J(\nu)$ = Single knife-edge diffraction loss estimate, given by (15)

$K_{h2} = 21.8 + 6.2 \log_{10}(f)$

$$J(\nu) = 6.9 + 20\log_{10}\left(\sqrt{(\nu - 0.1)^2 + 1} + \nu - 0.1 \right) \quad (15)$$

where:

$J(\nu)$ = Single knife-edge diffraction loss estimate

$\nu = K_{nu}\sqrt{h_{\text{diff}}\theta_{\text{clut}}}$

$h_{\text{diff}} = R - h$ (m)

$\theta_{\text{clut}} = \tan^{-1}\left(\frac{h_{\text{diff}}}{w_s}\right)$ (degrees)

$K_{nu} = 0.342\sqrt{f}$

f = Frequency (GHz)

w_s = Relates to width of street (m) default = 27

R = Representative clutter height (m)

h = Antenna height (m)

TABLE 11 ITU predicted extra clutter loss from Equation (14) for all considered environments and frequencies

Environment	VHF (dB)	UHF (dB)
Rural	12.1	17.7
Suburban	8.6	18.6
Urban	11.8	22.4
Dense urban	14.2	24.9

Abbreviation: ITU, International Telecommunication Union.

TABLE 12 RMSE between extra clutter loss inclusive models and the measured path-loss, including the change in RMSE between corrected and uncorrected models

	Free Space with clutter				Two ray with clutter			
	E_{RMS} (dB)		E_{dif} (dB)		E_{RMS} (dB)		E_{dif} (dB)	
Environment	VHF	UHF	VHF	UHF	VHF	UHF	VHF	UHF
Rural	25.8	46.2	−11.8	−17.5	17.6	13.2	5.7	−11.7
Suburban	28.8	45.5	−8.4	−18.3	5.9	17.2	−3.9	−17.4
Urban	33.1	38.9	−11.5	−21.9	15.8	18.8	−10.8	−21.1
Dense urban	25.0	37.0	−13.6	−24.5	11.7	19.3	−9.7	−23.7

Table 12 shows the RMSE (E_{RMS}) of both the free space path-loss model and the two ray model when additional clutter losses from Table 11 are incorporated in to each model, considered against the measurements taken in each environment at VHF and UHF. Using previous results shown in Tables 3, 4, 5 and 6, the cluttered and uncluttered free space RMSEs are compared to see if the RMSE to the measurements has been decreased by the addition of clutter to the model, and the same process is performed with the cluttered and uncluttered two ray models. The difference between cluttered and uncluttered for each model is noted in the table by E_{dif}, a negative difference suggests the RMSE has decreased and the model has therefore become more accurate, a positive difference suggests the RMSE has increased and therefore the model has become less accurate.

In almost all the scenarios considered, the addition of clutter loss increased the accuracy of the models predictions by a significant amount, which is shown by E_{imp} in Table 12, with the best case improving by 24.5 dB. This improvement is expected because clutter loss is a very important mechanism affecting propagation, so adding a consideration of its effects will produce a more complete model. However, none of the corrected free space models predictions came close to the

accuracy of the Hata or calculated models. The corrected two ray model performed better, especially at the UHF, where the accuracy was much better than the Hata models, but not as good as the calculated models.

4 | CONCLUSION

It has been shown that the current mainstream propagation models do not accurately predict the propagation loss of an IoT deployment at the frequencies of 71 and 869.525 MHz within rural, suburban, urban or dense urban environments with RX antennas deployed close to ground. It has also been shown that the propagation at these frequencies and within these environments can be accurately modelled using a conventional log-distance model with the correct parameters. Measured path-loss is shown to be consistently lower at VHF than UHF, meaning that even with the low efficiency helical antenna used in this study to simulate an IoT deployment, VHF retained its advantage for long distance communication in all the studied environments. Shadowing was shown to be close to predicted levels at VHF and UHF in all environments, with no frequency having a clear advantage. The recorded RF noise was measured and found to be consistently lower at UHF than VHF, and interesting differences were seen in the variation of individual noise measurements (shown by the standard deviation of the average noise), possibly relating to the time of day the measurements were taken. These results suggest that the newly repurposed VHF spectrum is suitable for IoT deployments in all the environments studied when compared to the currently utilised UHF spectrum.

Future work will attempt to measure the RF environment over a longer time period at static locations in order to discover if the RF noise, and indeed other propagation readings, has a time dependant factor to them possibly related to the intensity of human activity or other factors.

ORCID
D.P. Wright [ID] https://orcid.org/0000-0003-0703-8418
E.A Ball [ID] https://orcid.org/0000-0002-6283-5949

REFERENCES
1. Oracle: What is the internet of things (iot)?. https://www.oracle.com/uk/internet-of-things/what-is-iot.html. Accessed 16 January 2020
2. OFCOM: Vhf radio spectrum for the internet of things (2016). https://www.ofcom.org.uk/__data/assets/pdf_file/0029/78563/vhf-iot-statement.pdf. Accessed: 14 September 2017
3. Wright, D. P., Ball, E. A.: Highly portable software defined radio test bed for dual band propagation studies. In: The Loughborough antennas propagation conference (LAPC 2018), Loughborough University pp. 1–6 (2018)
4. Wright, D.P., Ball, E.A.: Highly portable, low-cost sdr instrument for RF propagation studies. IEEE Trans. Instrument. Measure. 69(8), 5446–5457 (2020)
5. Sigfox: Sigfox technology overview. https://www.sigfox.com/en/sigfox-iot-technology-overview. Accessed 13 September 2017
6. LoRa Alliance: What is LoRaWAN? (2015). https://docs.wixstatic.com/ugd/eccc1a_ed71ea1cd969417493c74e4a13c55685.pdf. Accessed 12 September 2017
7. Rappaport, T.S.: Wireless Communications: Principles and Practice. Prentice-Hall, Upper Saddle River (2002)
8. Dagefu, F.T., et al.: Short-range low-VHF channel characterization in cluttered environments. IEEE Trans. Antennas Propag. 63(6), 2719–2727 (2015)
9. Faruk, N., et al.: Clutter and terrain effects on path loss in the vhf/uhf bands. IET Microw. Antennas Propag. 12(1), 69–76 (2018)
10. Andrusenko, J., et al.: VHF General Urban Path Loss Model for Short Range Ground-to-Ground Communications. IEEE Transactions on Antennas and Propagation. 56(10), 3302–3310 (2008)
11. Devasirvatham, D.M.J., et al.: Multi-frequency radiowave propagation measurements in the portable radio environment IEEE International Conference on Communications, Including Supercomm Technical Sessions, vol. 4, pp. 1334–1340 (1990)
12. Fuschini, F., et al.: Analysis of Outdoor-to-Indoor Propagation at 169 MHz for Smart Metering Applications. IEEE Trans. Antennas Propag. 63(4), 1811–1821 (2015)
13. ETSI: Electromagnetic compatibility and Radio spectrum Matters (ERM); Short Range Devices (SRD); Radio equipment to be used in the 25 MHz to 1 000 MHz frequency range with power levels ranging up to 500 mW; Part 1: Technical characteristics and test methods (2012)
14. Ayadi, M., Ben Zineb, A., Tabbane, S.: A uhf path loss model using learning machine for heterogeneous networks. IEEE Trans. Antennas Propag. 65(7), 3675–3683 (2017)
15. Sarkar, T.K., Abdallah, M.N., Salazar-Palma, M.: Survey of available experimental data of radio wave propagation for wireless transmission. IEEE Trans. Antennas Propag. 66(12), 6665–6672 (2018)
16. El Chall, R., Lahoud, S., El Helou, M.: Lorawan network: radio propagation models and performance evaluation in various environments in Lebanon. IEEE IoT J. 6(2), 2366–2378 (2019)
17. Sandoval, R.M., Garcia-Sanchez, A., Garcia-Haro, J.: Improving RSSI-based path-loss models accuracy for critical infrastructures: a smart grid substation case-study. IEEE Trans. Ind. Informat. 14(5), 2230–2240 (2018)
18. Hejselbæk, J., et al.: Empirical study of near ground propagation in forest terrain for internet-of-things type device-to-device communication. IEEE Access. 6, 54052–54063 (2018)
19. Tewari, R.K., Swarup, S., Roy, M.N.: Radio wave propagation through rain forests of India. IEEE Trans. Antennas Propag. 38(4), 433–449 (1990)
20. Wang, W., Yang, L., Zhang, Q., Jiang, T.: Securing on-body IoT devices by exploiting creeping wave propagation. IEEE J. Select. Areas Commun. 36(4), 696–703 (2018)
21. ITU-R: Recommendation ITU-R P.525-3 Calculation of free-space attenuation (2016)
22. Goldsmith, A.: Wireless Comunications. Cambridge University Press, Cambridge (2005)
23. ITU-R: Recommendation ITU-R P.1406-2 Propagation effects relating to terrestrial land mobile and broadcasting services in the VHF and UHF bands (2015)
24. Silicon Labs: Si106X Delelopment Kits User's Guide (2017). https://www.silabs.com/documents/public/user-guides/Si106x-DK.pdf. Accessed 30 July 2020
25. Karedal, J., et al.: Path loss modeling for vehicle-to-vehicle communications. IEEE Trans. Vehicular Technol. 60(1), 323–328 (2011)
26. ITU.R: Recommendation ITU-R P.2108-0 Prediction of clutter loss (2017)